Colloids and Surfaces A: Physicochemical and Engineering Aspects 631 (2021) 127712

Contents lists available at ScienceDirect

Colloids and Surfaces A: Physicochemical and Engineering Aspects

journal homepage: www.elsevier.com/locate/colsurfa

The effect of protein BSA on the stability of lipophilic drug (docetaxel)-loaded polymeric micelles

H. Polat [a], M. Cevik Eren [a], M. Polat [b,*]

[a] Department of Chemistry, Izmir Institute of Technology, Urla, Izmir, Turkey
[b] Department of Chemical Engineering, Izmir Institute of Technology, Urla, Izmir, Turkey

HIGHLIGHTS

- Docetaxel-loaded micelles are stable for long time in DW and SBF solutions.
- The micelles disintegrate progressively with increasing BSA concentration.
- BSA concentration for complete disintegration is around the plasma HSA concentration.
- Presence of lipophilic docetaxel in micellar cores cannot prevent protein-induced disintegration.
- Changing docetaxel concentration in micellar cores cannot improve stability.

GRAPHICAL ABSTRACT

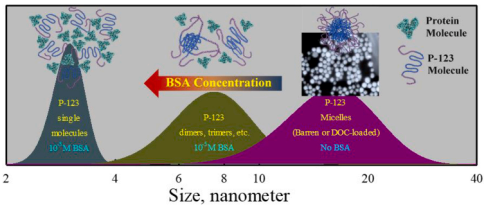

ARTICLE INFO

Keywords:
Drug-carriers(s)
Polymeric surfactants
Micelle(s)
Protein(s)
Docetaxel

ABSTRACT

Polymeric micelles are promising delivery vehicles for improving the efficacy of anticancer drugs and reducing their side effects. However, considering the binding ability of serum albumin, the possible interaction of micelles with the native plasma components in the bloodstream raises serious questions on micellar stability. The stability of barren or drug-loaded copolymeric micelles was investigated systematically in distilled water (DW) and simulated body fluid (SBF) solutions in the presence of a model protein. The copolymer was a Pluronic® series triblock copolymer (P-123), the drug was strongly lipophilic docetaxel (DOC) and the protein was Bovine Serum Albumin (BSA). The effect of such factors as BSA and DOC concentrations and the aging of the micellar solutions was studied. Both the barren and drug-loaded micelles were quite stable in blank DW and SBF solutions for long times up to 10 days. They lost integrity and showed no inclination to re-assemble when the BSA concentration reached a critical value, which was very close to the plasma Human Serum Albumin (HSA) concentration. The presence of DOC in the micellar cores could not prevent disintegration. The results illustrate clearly that ensuring the stability of polymeric micelles in blood plasma should be an important design factor in their use as drug carriers.

1. Introduction

Drug delivery systems allow clinicians to transport and deliver the active drug molecules to desired tissues, organs, cells, and subcellular organs more efficiently. Among the various delivery vehicles studied, micelles of polymeric surface-active agents are gaining popularity [1–3]. Micelles are core-shell structures formed by spontaneous aggregation of amphiphilic surfactant molecules in aqueous solutions above a certain

* Corresponding author.
E-mail address: mehmetpolat@iyte.edu.tr (M. Polat).

https://doi.org/10.1016/j.colsurfa.2021.127712
Received 18 August 2021; Received in revised form 27 September 2021; Accepted 5 October 2021
Available online 12 October 2021

Table 1
Basic properties of the chemicals employed in the study.

Name	Chemical structure	MW g/mole
Pluronic® copolymer (P-123)	$HO(EO)_{20}(PO)_{70}(EO)_{20}H$	5800
Docetaxel (DOC)	$C_{43}H_{53}NO_{14}$	807.9
Ethanol (EtOH)	C_2H_5OH	46.07
Bovin serum albumin (BSA)	Single polypeptide chain of 583 amino acid residues	66,463

concentration (the critical micelle concentration, CMC). In a micelle, the core section formed by the hydrophobic portions of the surfactant molecules offers an environment for dissolving and storing lipophilic active molecules [4–16] while the shell section is composed of hydrophilic components provides necessary solubility and response characteristics [17–22].

Plasma is the liquid component of blood that carries nutrients, hormones, and proteins to tissues while removing their metabolic waste products. It is composed of around 90% water and constitutes 55% of the blood volume. The remaining plasma components are salt ions, hormones, lipids, and proteins. Albumin, a protein synthesized by the liver at the rate of about 10–15 gm per day, embodies more than half of the total protein content of 60–80 g/L in human plasma. It is the main transport agent in the plasma due to its affinity for binding a variety of hydrophobic ligands such as fatty acids, lysolecithins, bilirubin, warfarin, tryptophan, steroids, anesthetics, and several dyes [23–25].

Micellization is a reversible process. Micelle integrity is influenced significantly when the solution surfactant concentration falls below the CMC. Kabanov et al. [26] remarked that dilution-related disintegration of the drug-bearing micelles may be responsible for diminishing the amount of drug which can be successfully transferred by the carrier. Polat et al. [27] demonstrated in a recent paper conclusively that diluting a fully-formed micellar system below a certain solution concentration resulted in total micelle disintegration.

The CMC of a given surface active agent, hence, the micelle stability, is also affected by pH, temperature, and presence of ionic species or other surface-active agents. Both the pH and temperature are relatively constant properties under physiological conditions. The effect of the presence of native plasma components on micelle stability, however, can not be overlooked. It is well known that proteins that are composed of various hydrophilic and hydrophobic amino acids display high surface activity and tend to strongly accumulate at the interfaces [28,29]. Therefore, the stability may be strongly influenced by the interaction of micelles, or of the highly lipophilic molecules they may envelop, with the plasma proteins [28–31]. Zhang et al. [3] report that the drug-loading capacity and formulation stability of the micellar carrier systems are less than satisfactory in clinical applications, an issue which is emphasized in other excellent reviews on micellar stability [32–35]. Despite such indications, studying micelle stability has been limited to model systems due to the difficulties in discriminating micelles from the native plasma species [32,34,36–51].

This paper aims at systematically quantifying the effect of the presence of protein molecules on the stability of copolymeric micelles in situ. The tests were carried out with barren and strongly lipophilic drug-loaded micelles in distilled water and simulated body fluids in the absence and presence of a model protein.

2. Materials

The micelles were formed using a Pluronic® series triblock copolymer (P-123). This copolymer is composed of two hydrophilic polyethylene blocks attached to a hydrophobic polypropelene block (PEO_{20}-PPO_{70}-PEO_{20}). It is commercially available and offers excellent biocompatibility as well as providing a more receptive environment for the lipophilic drug molecules due to the longer hydrophobic blocks [52,53]. Docetaxel (DOC) was employed as the drug due to its strong lipophilic nature and water insolubility. It has a logP of 4.1 and Pka of 10.97, which results in poor aqueous solubility (0.025 μg/ml) and low membrane permeability (10^{-6} cm/s) [54]. Bovine Serum Albumin (BSA) was used as the model protein. This large globular protein is a homolog of Human Serum Albumin (HSA) with similar ligand-binding affinities [55]. It is negatively charged in water up to pH 4.7 and is readily soluble in water. Ethanol (EtOH) was used as the co-solvent for the drug and the block copolymer. All chemicals (Table 1) were supplied by Sigma Aldrich (Turkey).

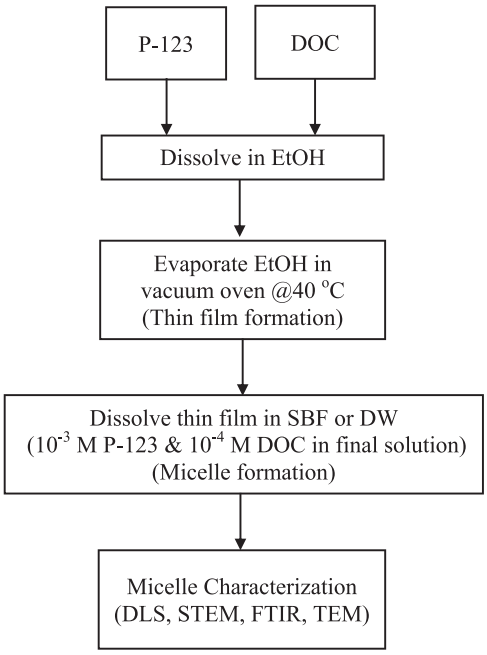

Fig. 1. The method employed for forming the micelles.

Simulated body fluid (SBF) is an electrolyte solution with an ionic strength similar to that of the human blood plasma. It was prepared by dissolving reagent grade chemicals of NaCl (7.996 g), $NaHCO_3$ (0.350 g), KCl (0.224 g), $K_2HPO_4{\cdot}3H_2O$ (0.228 g), $MgCl_2{\cdot}6H_2O$ (0.305 g), $CaCl_2{\cdot}2H_2O$ (0.278 g) and Na_2SO_4 (0.071 g) in about 500 ml L of deionized water. The reagents were dissolved one by one in the order as given in the previous sentence after the former reagent was completely dissolved. Trishydroxymethyl aminomethane $(CH_2OH)_3CNH_2$ (6.570 g) was dissolved in 1 M-HCl solution (40 ml, about 90% of the total HCl to be added) for buffering and then added to the main solution. The temperature of the solution was adjusted to 36.5 °C with a water bath and the solution was titrated to pH 7.4 with 1 N-HCl. Finally the total volume was adjusted to 1 L [56].

3. Micelle formation and characterization

DOC loading was done by a modified thin-film hydration method [27]. P-123 was co-dissolved with the drug in an excess amount of EtOH followed and the solvent was evaporated. The residue was an organic film of the polymer-drug composite which was subsequently hydrated in water or SBF to have respective surfactant and drug concentrations of 10^{-3} M and 10^{-4} M. The thin film method energetically forces the lipophilic drug molecules into micelles which subsequently dissolve in the aqueous phase. A schematic flowsheet of the procedure is presented in Fig. 1.

The size and surface charge of the micelles were measured in-situ in solution using Dynamic Light Scattering (DLS) and Dynamic Light Scattering with Laser Doppler Velocimetry (DLS-LDV, Malvern Panalytical, UK). The size distribution measurements were repeated

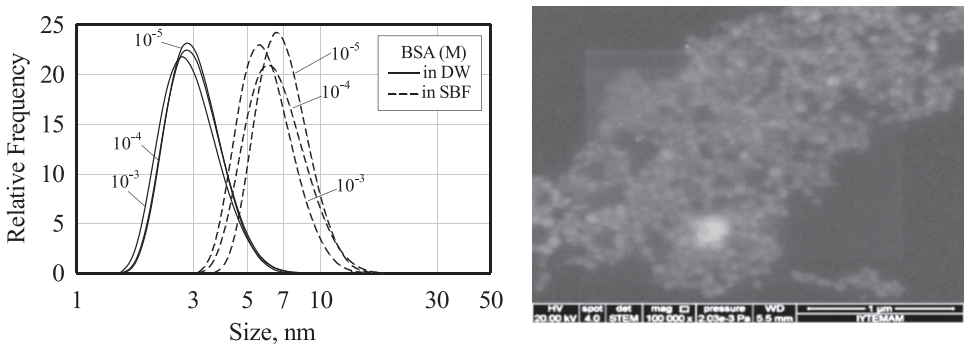

Fig. 2. In-situ size distributions of the BSA molecules in DW and SBF solutions (left) and STEM picture of BSA in DW (right).

multiple times until a stable size distribution curve was obtained, by preparing a new fresh micelle solution if necessary. The distributions reported are the results of those stable distributions. Moreover, such a stable size distribution measurement is an average of the 3 repeats the device automatically carries out. Since such size distribution curves are very close, only the average of the three is presented for clarity.

Micelle morphology was observed by Scanning Transmission Electron microscopy (STEM, FEI Quanta^{TM} 250 FEG, USA) under vacuum after drying an aliquot of the micelle solution on carbon grids. A carbon grid is a flat disc which contains holes on which a thin section of a specimen is placed. The holes in the grids allow the electrons to pass through the specimen and provide a better detail.

Fourier Transform Infrared Spectroscopy (FTIR, Perkin Elmer Spectrum Two U-ATR, USA) was employed using for indirectly determining how micelles, proteins, and the drug molecules interact. The Universal Attenuated Total Reflectance Accessory (UATR) is an internal reflection accessory, used for simplifying the analysis of solids, powders, pastes, gels and liquids. In this technique, a sample is placed on top of a crystal with a high refractive index. An infrared beam from the instrument is passed into the accessory and up into the crystal. It is then reflected internally in the crystal, and back towards the detector which is housed in the instrument. When the beam is reflected within the crystal, it penetrates into the sample by a few microns.

4. Results and discussions

4.1. Characterization of BSA

BSA is a globular protein with dimensions 4 × 4 × 14 nm with an equivalent volume diameter of 6.1 nm [57]. Being a biological homolog of HSA with similar ligand-binding properties, it is widely employed as a replacement in many biochemical and pharmacological applications [54,58,59].

Left-hand-side graphs in Fig. 2 present in-situ size distributions of the protein molecules in DW and SBF at 10^{-5}, 10^{-4} and 10^{-3} M BSA concentrations. The mean size does not change appreciably with concentration and is around 3.0 nm in DW, which is in agreement with the literature reported values [57,60,61]. The size of the molecules are larger in SBF solutions as predicted by Curtis et al. [62] who reported that high salt concentrations should lead to aggregation of the protein molecules. The slight decrease in size at higher BSA concentrations could be caused by the compaction of the protein molecules due to double-layer compression. A STEM photograph given in the right-hand-side of Fig. 2 shows that the protein molecules in DW have the expected globular morphology.

Since the isoelectric point (IEP) of BSA is known to be between pH 4.5–5.0, it is negatively charged at neutral pH [27,63–65]. We observed using DLS-LDV that the mean surface charge was − 25 mV in DW at natural pH and shifted to zero in SBF solution, most probably due to suppression of the double layer around the molecule at high salt content. This supports the aggregation-related size increase observed in SBF solutions mentioned above.

4.2. Characterization of barren (unloaded) P-123 micelles

4.2.1. In the absence of BSA

Barren micelles formed in DW and SBF solutions which contain 10^{-3} M P-123 were characterized using DLS and STEM. Fig. 3 (left) presents the size distribution of the fresh micelles in DW and SBF solutions. The mean micelle size is around 16 nm in both cases, which is in good agreement with previous observations [27,66–70]. The spherical shapes of the micelles can be clearly observed in the STEM photograph also given in Fig. 3 (right). Size distribution of the micelles did not change significantly after 10 days of aging under ambient conditions, indicating that the micelles were quite stable both in DW and SBF.

Zeta potential measurements of the P-123 micelles showed that the charge distribution of the micelle population was wider in DW (between −40 and +40 mV) with the mean zeta potential lying around zero, most probably due to the average non-ionic nature of the co-polymer [27]. The charge distribution became narrower in the SBF solution (between

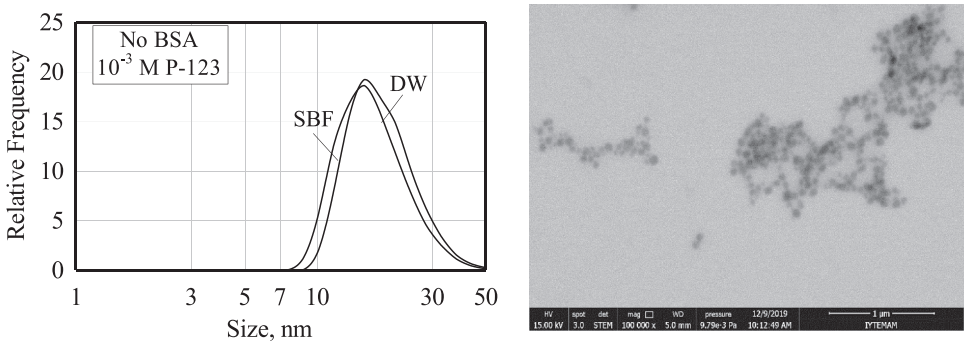

Fig. 3. In-situ size distributions of the fresh barren P-123 micelles (10^{-3} M) in DW and SBF solutions (left) and STEM images of the barren micelles in DW (right).

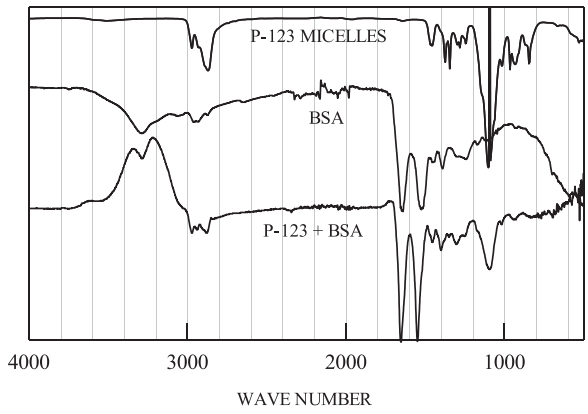

Fig. 4. FTIR spectra of P-123 micelles and the BSA separately and when they are together in DW solution.

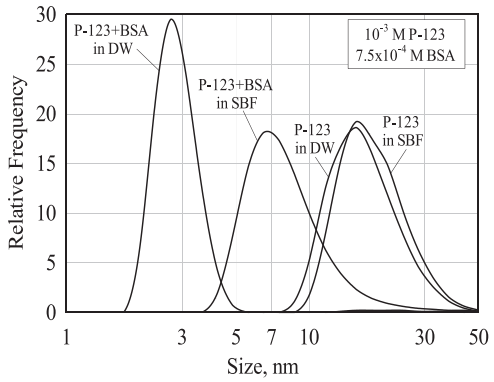

Fig. 5. Size distributions of the barren P-123 micelles (10^{-3} M) in-situ in DW and SBF solutions in the absence and presence of 7.5×10^{-4} M BSA.

−20 and +20 mV) and the mean charge shifted to − 10 mV. This behavior was similar to that previously observed with Pluronic® F-68 in the literature [70]. The reason for the narrowing of the distribution can be attributed to the suppression of the double layer around the molecule in the SBF solution. The shift to the negative side may have been caused by asymmetric folding of the positively and negatively charged sections of the molecule during such suppression.

4.2.2. In the presence of BSA

The FTIR spectra of the P-123 micelles and BSA and of a BSA + P-123 solution in DW are presented in Fig. 4. It can be seen that P-123 shows strong peaks corresponding to the C-H stretching and bending vibrations in 2850–3000 cm^{-1} range and at 1460 cm^{-1}. The peaks at 1377 and 1350 cm^{-1} are assigned to the stretching modes of C-O-C on P-123. For BSA, the major characteristic peak at 3299, 1656, and 1535 cm^{-1} are assigned to the stretching vibration of O-H, amide I, and amide II bands, respectively. When the spectra of the P-123 micelles is obtained in the presence of BSA, it can be seen that both the P-123 and the BSA peaks are clearly visible. This indicates that the interactions between the P-123 micelles and BSA molecules do not include chemical bonding, as suggested by Liu et al. [30].

An aliquot of protein solution was injected into fresh DW and SBF micelle solutions such that a final BSA concentration of 7.5×10^{-4} M was obtained without causing appreciable dilution. The BSA concentration selected was within the range of plasma protein concentration of 5×10^{-4} M to 9×10^{-4} M. Fig. 5 presents the size distribution of the fresh micelles following protein injection along with the size distribution of the micelles when there was no BSA (from Fig. 3).

Fig. 5 shows plainly that when the fully-formed barren micelles in DW or SBF solutions are brought in contact with the BSA molecules, there is a significant reduction in micelle size. The reduction is much more pronounced in DW (from 16 to around 3 nm) compared to that in SBF (from 16 to around 7 nm).

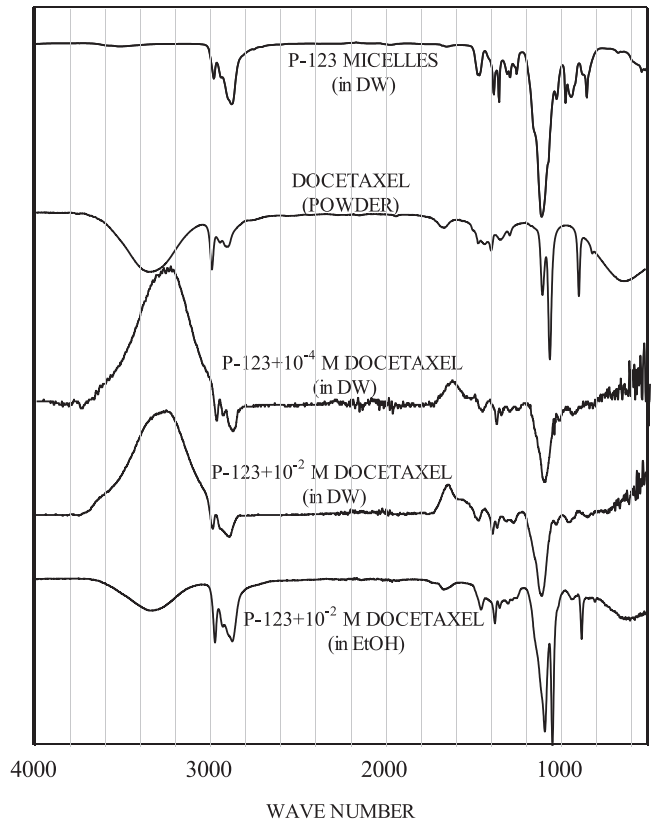

Fig. 6. FTIR spectra of P-123 micelles, DOC and DOC-loaded P-123 micelles in DW and EtOH.

It should be noted at this point that size of the P-123 monomers cannot be reliable observed with the DLS technique. The signal never stabilizes into a well-defined distribution curve, most probably due to the dynamic anisotropic geometry of the monomers. Hence, the well-defined distribution curve with the mean size of 3 nm is probably the signal from the globular BSA molecules (see Fig. 2), indicating that the micelles have been completely disintegrated into monomers when they co-exist with BSA in DW. The size distribution in SBF reinforces this observation. The micelle size of 16 nm observed in blank SBF solutions is reduced to around 7 nm when the micelles are brought into contact with the protein molecules. Since 7 nm is the mean size of the protein molecules in the SBF solutions (see Fig. 2), it is obvious that the presence of protein molecules causes complete micelle disintegration into monomer species in the SBF solutions as well. We observed that aging the protein-doped micellar solutions up to 10 days did not lead to any re-assembling of the surfactant molecules once disintegrated in the presence of the protein molecules.

In another test, the micelles were formed by placing the P-123 thin films directly in protein solutions instead of injecting the protein into pre-formed micelle solutions. The fact that no micelle formation could not be observed illustrates that micelles cannot even begin to form in the presence of protein molecules.

These results show that the presence of a specific concentration of BSA has a destructive effect on micelle integrity. Whether the presence of strongly hydrophobic drug molecules in the micellar core can mitigate this effect will be discussed in the following sections.

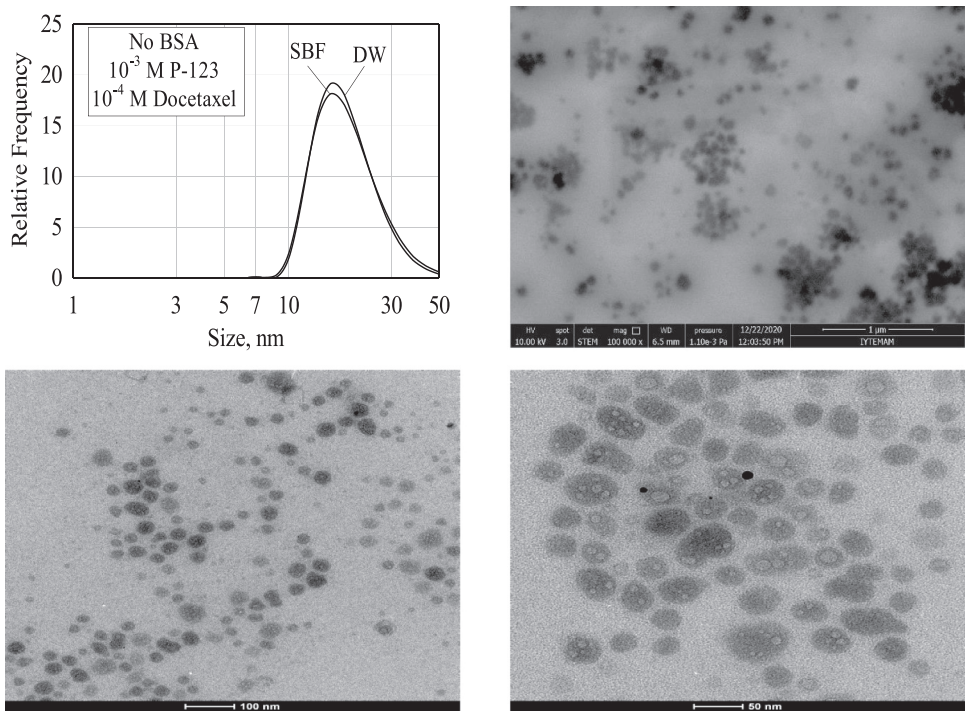

Fig. 7. In-situ size distributions of the DOC-loaded (10^{-4} M) P-123 micelles (10^{-3} M) in DW and SBF solutions 1 h after they have been formed (left) and STEM images of the loaded micelles in DW (right). TEM pictures of the drug-loaded micelles in a greater detail in DW (bottom raw left and right).

4.3. Characterization of DOC-loaded P-123 micelles

A strongly hydrophobic anticancer drug (DOC) was encapsulated within the P-123 micelles by the modified thin-film hydration method described. The final concentration of the drug in the micellar solution was fixed at 10^{-4} M unless intentionally varied. The spectra of the P-123 micelles and DOC are presented in Fig. 6. DOC gave a broadband at 3331 cm^{-1} due to N—H bond and O—H bond overlapping and a peak around 2972 cm^{-1} due to C-H stretching. Also, a characteristic C═C bending vibration at 800 cm^{-1} can be clearly observed. Furthermore, the drug displays another strong C-O stretch peak at around 1050 cm^{-1}. The spectrum of P-123 micelles in water, loaded with 10^{-4} M and 10^{-2} M DOC, displayed the major P-123 peak between 1000 and 1100 cm^{-1} strongly. It is important to note that the DOC C═C bending peak at 800 cm^{-1} and C-O stretch peak at around 1050 cm^{-1} have completely disappeared when the micelles were in water. Actually, the spectrum of the DOC-loaded P-123 micelles did not show any characteristic peaks related to the drug, suggesting that DOC was encapsulated in the micelle structure. The figure gives the spectrum of the same DOC-loaded P-123 micelles after they have been placed in EtOH solution. It is obvious that the micelle disintegration in EtOH should lead to the release of the encapsulated DOC molecules if any is present in the micelle structure. The spectra display the characteristic DOC C═C bending vibration peaks at 800 cm^{-1} and the C-O stretch peaks at 1050 cm^{-1} also appear along with the characteristic P-123 peaks. These observations are further indications of the successful encapsulation of the drug molecules within the P-123 micelles.

4.3.1. In the absence of BSA

The size distributions of the fresh DOC-loaded micelles in DW and SBF solutions are presented in Fig. 7 (top raw left) in the absence of BSA. It can be seen that the behavior of the drug-loaded micelles is very similar to that of the barren micelles for both the DW and SBF solutions (see Fig. 3). Further testing showed that the size of the micelles was observed to be constant with aging up to 10 days in both DW and SBF solutions. A STEM photograph of the DOC-loaded fresh micelles in DW solution in the absence of BSA is also presented in Fig. 7 (top raw right). Fig. 7 also presents the TEM pictures of the drug-loaded micelles in a greater detail (bottom raw left and right).

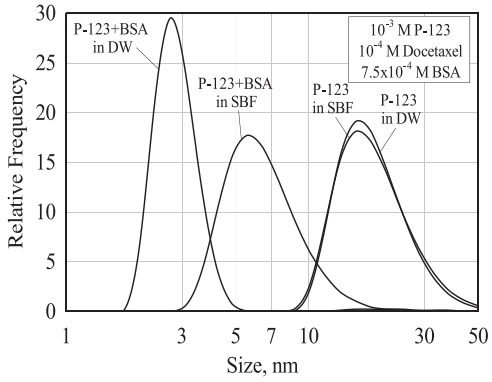

Fig. 8. Size distributions of the docetaxel-loaded (10^{-4} M) P-123 micelles (10^{-3} M) in-situ in DW and SBF solutions in the absence and presence of 7.5×10^{-4} M BSA.

4.3.2. In the presence of BSA

Similar to the case with the barren micelle solutions, an aliquot of a protein solution was injected into fresh DOC-loaded micelle solutions to have a final BSA concentration of 7.5×10^{-4} M. Care was taken that the addition of the protein solution did not cause appreciable dilution in the micellar solution. Fig. 8 presents the size distribution of the fresh drug-loaded micelles following protein injection in DW and SBF solutions along with the size distribution of the drug-loaded micelles in the absence of BSA from Fig. 7. The figure displays clearly that the addition of the protein causes drug-loaded micelles to disintegrate and that the behavior is very similar to that observed with the barren micelles (see Fig. 5). It is obvious that micelles disintegrate when a certain protein concentration is present even in the presence of a strongly lipophilic drug in the micellar cores.

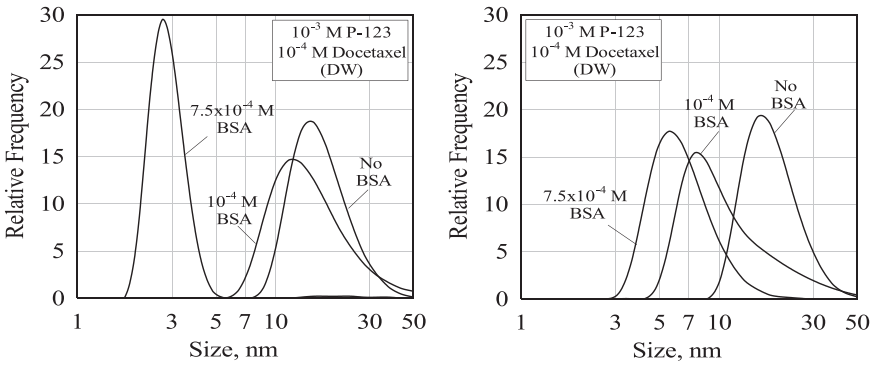

Fig. 9. Size distributions of the DOC-loaded (10^{-4} M) P-123 micelles (10^{-3} M) in-situ in DW (left) and in SBF (right) solutions in the presence of varying concentrations of BSA.

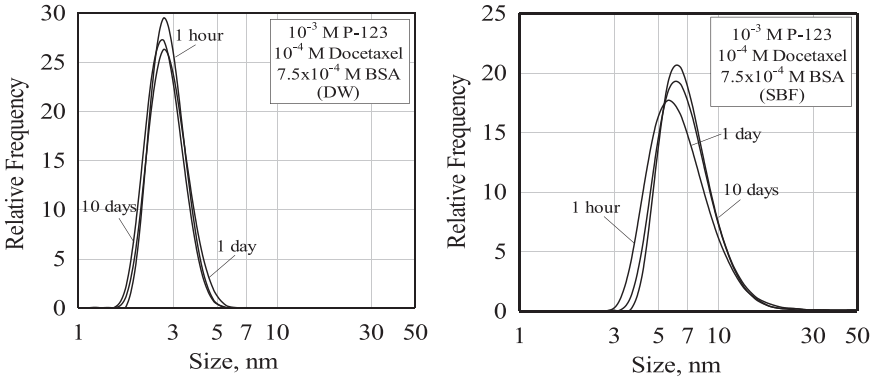

Fig. 10. Size distributions of the DOC-loaded (10^{-4} M) P-123 micelles (10^{-3} M) in-situ in DW (left) and in SBF (right) solutions in the presence of 7.5×10^{-4} M BSA as a function of the age of the micellar solutions.

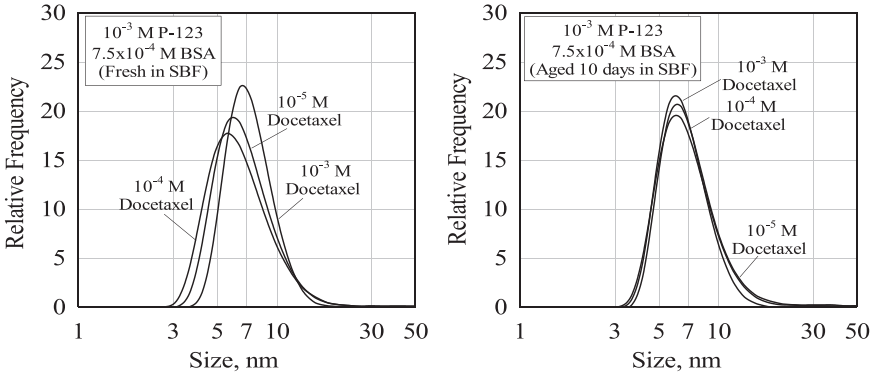

Fig. 11. Size distributions of the DOC-loaded (10^{-4} M) fresh (left) and aged (right) P-123 micelles (10^{-3} M) in-situ in SBF solutions in the presence of 7.5×10^{-4} M BSA as a function of varying DOC concentrations.

The effect of the protein was tested further by varying the amount of BSA in DW and SBF solutions and the results are presented in Fig. 9. The tests were carried out at several protein concentrations ranging between 10^{-6} to 10^{-3} M, changing. The data for 10^{-5} and 10^{-6} M BSA were very close to that of the no BSA case and are not shown in the figures for clarity. For the DW case (left), the presence of low concentration of BSA (10^{-4} M) does not cause a significant micelle disintegration but increasing the BSA concentration to 7.5×10^{-4} M completely disintegrates the micelles. It seems that the presence of the protein has a drastic effect on micelle integrity after a critical protein concentration is reached. For the case of SBF, the effect seems to be more gradual, but the micelles still completely disintegrate at the BSA concentration of 7.5×10^{-4} M. Fig. 10 gives the size distribution of the drug-loaded micelles which have disintegrated at the BSA concentration of 7.5×10^{-4} M (see Fig. 9) after 10 days of aging. It can be seen that the aging of the micelles did not bring about reaggregation or any appreciable change in size.

The effect of the BSA on the micelle integrity was tested further at varying DOC loading amounts between 10^{-3} M and 10^{-5} M for fresh micelles and the results are presented in the left-hand-side graphs in Fig. 11. The figure shows that the micelle break-up takes place even when the concentration of the strongly lipophilic DOC was increased or decreased by 10-fold. The right-hand-side graph in Fig. 11 gives the size distributions of the same solutions after 10 days of aging. It can be seen that the drug-loaded micelles behave similarly to the barren.

It is obvious from these results that the presence of BSA disrupts the

micelle integrity even in the presence of the strongly hydrophobic drug molecules in the micellar core. The data suggests that the disintegrated micelles do not show any re-aggregation with time if BSA is present. They further show that the presence of a hydrophobic drug present in the micellar core does not have an appreciable effect in preventing disintegration even at high concentrations. The fact that the BSA concentration which leads to disintegration is close to the plasma HSA concentration suggests that a similar disruption is quite possible in actual applications of micellar drug carriers.

5. Conclusions

In this study, the effect of the protein BSA on the stability of the barren and DOC-loaded P-123 micelles was investigated in DW and SBF solutions under changing protein and drug concentrations and at different aging times. Characterization tests were carried out employing DLS measurements, STEM imaging, and FTIR analysis. The study demonstrated clearly that:

- The barren and DOC-loaded micelles are quite stable in DW and SBF solutions when there are no protein molecules.
- Introduction of protein molecules into micellar solutions affects micelle stability in DW or SBF solutions significantly. The micelles disintegrate completely when the protein concentration in the solution is around 10^{-3} M.
- Protein-induced micelle disintegration can take place in the absence of any dilution. The disintegrated micelles show no inclination to re-assemble in concentrated protein solutions for long times.
- The presence of a strongly lipophilic drug (DOC) in the micellar cores cannot prevent micelle disintegration irrespective of the drug concentration once the protein concentration reaches around 10^{-3} M.
- The protein concentration where micelles disintegrate is close to the HSA concentration in blood plasma. Therefore, the stability of polymeric micelles as drug carriers should be serious concern in the presence of native plasma components and must be aided by some other means of protection to assure stability.
- The interaction between the protein molecules and the micelles seems to be physical. The micelle break up above a certain protein concentration may be due to physical factors such as protein molecules interfering with the micellization/de-micellization process.

The paper shows conclusively with a model amphiphilic block copolymer that presence of protein molecules can affect micelle stability significantly. Combined with the information that dilution also causes micelle break up [27], the results point out to the possible reasons for the less-than-expected efficiency of micellar drug carriers. The work could be pursued further to determine the degree to which the drug is freed, the possible means to inhibit such disintegration (grafting, encapsulation, etc.) and the mode of interaction between the micelles and the protein molecules by other methods such as atomic force microscopy, molecular simulations, etc.

CRediT authorship contribution statement

Hurriyet Polat: Conceptualization, Methodology, Writing – original draft, Supervision. **Merve Cevik Eren:** Investigation. **Mehmet Polat:** Resources, Writing – review & editing, Visualization, Project administration.

Declaration of Competing Interest

The authors declare that they have no known competing financial interests or personal relationships that could have appeared to influence the work reported in this paper.

Acknowledgments

The authors appreciate the financial support from IZTECH (Izmir Institute of Technology, Turkey) Research Fund. They also thank Specialist Mutlu Yaman of the Material Research Center (IZTECH) for performing STEM analyses and Specialist Yekta Gunay Atli of the Biotechnology and Bioengineering Application and Research Center (IZTECH) for helping with the FTIR analyses.

References

[1] C. Li, J. Wang, Y. Wang, H. Gao, G. Wei, Y. Huang, H. Yu, Y. Gan, Y. Wang, L. Mei, H. Chen, H. Hu, Z. Zhang, Y. Jin, Recent progress in drug delivery, Acta Pharm. Sin. B 9 (2019) 1145–1162.
[2] H.S. Kapare, S.R. Metkar, Micellar drug delivery system: a review, Pharm. Reson. (2020) 2.
[3] Y. Zhang, Y. Huang, S. Li, Polymeric micelles: nanocarriers for cancer-targeted drug delivery, AAPS PharmSciTech 15 (2014) 862–871.
[4] P. Linse, M. Malmsten, Temperature-dependent micellization in aqueous block copolymer solutions, Macromolecules 25 (1992) 5434–5439.
[5] K. Mortensen, W. Brown, B. Norden, Inverse melting transition and evidence of 3-dimensional cubatic structure in a block-copolymer micellar system, Phys. Rev. Lett. 68 (1992) 2340–2343.
[6] P. Alexandridis, T. Alan Hatton, Poly(ethylene oxide)-poly(propylene oxide)-poly (ethylene oxide) block copolymer surfactants in aqueous solutions and at interfaces: thermodynamics, structure, dynamics, and modeling, Colloids Surf. A 96 (1995) 1–46.
[7] P. Alexandridis, Poly(ethylene oxide) poly(propylene oxide) block copolymer surfactants, Curr. Opin. Colloid Interface Sci. 2 (1997) 478–489.
[8] H. Polat, S. Chander, Adsorption of PEO/PPO triblock copolymers and wetting of coal, Colloids Surf. A 146 (1999) 199–212.
[9] P. Verrna, S. Nath, P.K. Singh, M. Kurnbhakar, H. Pal, Effects of block size of Pluronic polymers on the water structure in the corona region and its effect on the electron transfer reactions, J. Phys. Chem. B 112 (2008) 6363–6372.
[10] A. Sturcova, P. Schmidt, J. Dybal, Role of hydration and water coordination in micellization of Pluronic block copolymers, J. Colloid Interface Sci. 352 (2010) 415–423.
[11] X.B. Xiong, A. Falamarzian, S.M. Garg, A. Lavasanifar, Engineering of amphiphilic block copolymers for polymeric micellar drug and gene delivery, J. Control. Release 155 (2011) 248–261.
[12] Y. Kadam, U. Yerramilli, A. Bahadur, P. Bahadur, Micelles from PEO-PPO-PEO block copolymers as nanocontainers for solubilization of a poorly water soluble drug hydrochlorothiazide, Colloids Surf. B: Biointerfaces 83 (2011) 49–57.
[13] W. Zhang, Y. Shi, Y. Chen, J. Ye, X. Sha, X. Fang, Multifunctional Pluronic P-123/F127 mixed polymeric micelles loaded with paclitaxel for the treatment of multidrug resistant tumors, Biomaterials 32 (2011) 2894–2906.
[14] M. Zhang, M. Djabourov, C. Bourgaux, K. Bouchemal, Nanostructured fluids from Pluronic® mixtures, Int. J. Pharm. 454 (2013) 599–610.
[15] E.S. Lee, Y.T. Oh, Y.S. Youn, M. Nam, B. Park, J. Yun, J.H. Kim, H.-T. Song, K. T. Oh, Binary mixing of micelles using Pluronics for a nano-sized drug delivery system, Colloids Surf. B Biointerfaces 82 (2011) 190–195.
[16] H. Zhiqi, H.P. Alexandridis, Micellization thermodynamics of Pluronic P-123 (EO20PO70EO20) amphiphilic block copolymer in aqueous ethylammonium nitrate (EAN) solutions, Polymers 10 (2018) 32.
[17] J.H. Park, S. Lee, J.H. Kim, K. Park, K. Kim, C. Kwon, Polymeric nanomedicine for cancer therapy, Prog. Polym. Sci. 33 (2008) 113–137.
[18] S. Deshayes, H. Cabral, T. Ishii, Y. Miura, S. Kobayashi, T. Yamashita, N. Nishiyama, K. Kataoka, Phenylboronic acid-installed polymeric micelles for targeting sialylated epitopes in solid tumors, J. Am. Chem. Soc. 135 (2013) 15501–15507.
[19] C. Shi, X. Guo, Q. Qu, Z. Tang, Y. Wang, S. Zhou, Actively targeted delivery of anticancer drug to tumor cells by redox-responsive star-shaped micelles, Biomaterials 35 (2014) 8711–8722.
[20] X. Jin, P. Zhang, L. Luo, H. Cheng, Y. Li, T. Du, B. Zou, M. Gou, Efficient intravesical therapy of bladder cancer with cationic doxorubicin nanoassemblies, Int. J. Nanomed. 11 (2016) 4535–4544.
[21] R.N. Gilbreth, S. Novarra, L. Wetzel, S. Florinas, H. Cabral, K. Kataoka, J. Rios-Doria, R.J. Christie, M. Baca, Lipid- and polyion complex-based micelles as agonist platforms for TNFR superfamily receptors, J. Control. Release 234 (2016) 104–114.
[22] P. Kumari, O.S. Muddineti, S.V.K. Rompicharla, Cholesterol-conjugated poly (D, L-lactide)-based micelles as a nanocarrier system for effective delivery of curcumin in cancer therapy, Drug Deliv. 24 (2017) 209–223.
[23] H.D. Carter, J.X. Ho, Advances in Protein Chemistry, Academic Press, New York, 1994, pp. 153–203.
[24] I.T. Kosa, T. Maruyama, M. Otagiri, Species differences of serum albumins: I. Drug binding sites, Pharm. Res. 14 (1997) 1607–1612.
[25] J.F. Moreno, M. Cortijo, J.G. Jimenez, Interaction of acrylodan with human serum albumin. A fluorescence spectroscopic study, Photochem. Photobiol. 69 (1999) 8–15.
[26] A.V. Kabanov, E.V. Batrakova, V.Y. Alakhov, Pluronic block copolymers as novel polymer therapeutics for drug and gene delivery, J. Control. Release 82 (2002) 189–212.

[27] H. Polat, G. Kutluay, M. Polat, Analysis of dilution induced disintegration of micellar drug carriers in the presence of inter and intra micellar species, Colloids Surf. A: Physicochem. Eng. Asp. 601 (2020) 1–9.
[28] S.M. Singh, S. Bandi, D.N.M. Jones, K.M.G. Mallela, Effect of polysorbate 20 and polysorbate 80 on the higher order structure of a monoclonal antibody and its fab and Fc fragments probed using 2D NMR spectroscopy, J. Pharm. Sci. 106 (12) (2017) 3486–3498, https://doi.org/10.1016/j.xphs.2017.08.011.
[29] H. Neurath, H.B. Bull, The surface activity of proteins, Chem. Rev. 23 (1938) 391–435.
[30] J. Liu, F. Zeng, C. Allen, Influence of serum protein on polycarbonate-based copolymer micelles as a delivery system for a hydrophobic anti-cancer agent, J. Control. Release 103 (2005) 481–497.
[31] K. Nešporová, J. Šógorkováa, D. Šmejkalováa, J. Kulháneka, G. Huerta-Angelesa, L. Kubalab, V. Velebnýa, Influence of serum albumin on intracellular delivery of drug-loaded hyaluronan polymeric micelles, Int. J. Pharm. 511 (2016) 638–647.
[32] S.C. Owen, C.P.Y. Dianna, M.S. Shoichet, Polymeric micelle stability, Nano Today 7 (2012) 53–65.
[33] J. Chen, Y.D. Ma, L.C. Wang, W.Y. Han, Preparation of chitosan/SiO2-loaded graphene composite beads for efficient removal of bilirubin, Carbon 143 (2019) 352–361.
[34] Y. Shi, T. Lammers, G. Storm, W.E. Hennink, Physico-Chemical Strategies to Enhance Stability and Drug Retention of Polymeric Micelles for Tumor-Targeted Drug Delivery, Macromol. Biosci. 17 (1) (2017) 41234, https://doi.org/10.1002/mabi.201600160.
[35] W. Zhou, C. Li, Z. Wang, W. Zhang, J. Liu, Factors affecting the stability of drug-loaded polymeric micelles and strategies for improvement, J. Nanopart. Res. 18 (2016) 275–293.
[36] J. Yaneva, S.H. Leuba, K. Van Holde, J. Zlatanova, The major chromatin protein histone H1 binds preferentially to cis-platinum- damaged DNA (anticancer drugsyDNA adductsyHMG1ylinker histones), Proc. Natl. Acad. Sci. 94 (1997) 13448–13451.
[37] Y. Jiang, C. Zhu, L. Ling, L. Wan, X. Fang, C. Bai, Specific aptamer-protein interaction studied by atomic force microscopy, Anal. Chem. 75 (2003) 2112–2116.
[38] G. Wang, Z. Nikolovska-Coleska, C.Y. Yang, R. Wang, G. Tang, J. Guo, S. Shangary, S. Qiu, W. Gao, D. Yang, J. Meagher, J. Stuckey, K. Krajewski, S. Jiang, P.P. Roller, H. Ozel Abaan, Y. Tomita, S. Wang, Structure- based design of potent Small-molecule inhibitors of anti-apoptotic Bcl-2 proteins, J. Med. Chem. 49 (2006) 6139–6142.
[39] J. Xu, Y. Li, Discovering disease-genes by topological features in human protein–protein interaction network, Oxf. J. 22 (2006) 2800–2805.
[40] Y.D. Ivanov, P.A. Frantsuzov, A. Zöllner, N.V. Medvedeva, A. Archakov, W. Reinle, R. Bernhardt, Atomic Force Microscopy Study of protein–protein interactions in the cytochrome CYP11A1 (P450scc)-containing steroid hydroxylase system, Nanoscale Res. Lett. 6 (2011) 54.
[41] T. Ando, T. Uchihashi, N. Kodera, A. Miyagi, R. Nakakita, H. Yamashita, M. Sakashita, High-speed atomic force microscopy for studying the dynamic behavior of protein molecules at work, Jpn. J. Appl. Phys. 45 (2006) 1–3.
[42] E.Y. Mayyas, Investigation of Protein-Protein Interaction Using Atomic Force Microscopy (Ph.D. dissertation), Nanomechanics Laboratory, Department of Physics and Astronomy, Wayne State University, Detroit, 2011.
[43] F.S. Kao, W. Ger, Y.R. Pan, H.C. Yu, R.Q. Hsu, H.M. Chen, Chip-based protein–protein interaction studied by atomic force microscopy, Biotechnol. Bioeng. 109 (2012) 2460–2467.
[44] M. Tribout, S. Paredes, M.J. González-Mañas, F.M. Goñi, Binding of triton X-100 to bovine serum albumin as studied by surface tension measurements, J. Biochem. Biophys. Methods 22 (1991) 129–133.
[45] W. Kevin, P. Mattison, L. Dubin, I.J. Brittain, Complex formation between bovine serum albumin and strong polyelectrolytes: effect of polymer charge density, J. Phys. Chem. B 102 (1998) 3830–3836.
[46] A. Valstar, M. Almgren, W. Brown, M. Vasilescu, The interaction of bovine serum albumin with surfactants studied by light scattering, Langmuir 16 (2000) 922–927.
[47] S.F. Santos, D. Zanette, H. Fischer, R. Itri, A systematic study of bovine serum albumin (BSA) and sodium dodecyl sulfate (SDS) interactions by surface tension and small angle X-ray scattering, J. Colloid Interface Sci. 262 (2003) 400–408.
[48] S. Bianca, Z. Dino, I. Rosangela, Bovine serum albumin (BSA) plays a role in the size of SDS micelle-like aggregates at the saturation binding: the strength effect, J. Colloid Interface Sci. 277 (2004) 285–291.
[49] C.L. Mesa, Polymer–surfactant and protein–surfactant interactions, J. Colloid Interface Sci. 286 (2005) 148–157.
[50] P. Opanasopit, M. Yokoyama, M. Watanabe, K. Kawano, Y. Maitani, T. Okano, Influence of serum and albumins from different species on stability of camptothecin-loaded micelles, J. Control. Release 104 (2005) 313–321.
[51] É. Kiss, K. Dravetzky, K. Hill, E. Kutnyánszky, A. Varga, Protein interaction with a Pluronic-modified poly(lactic acid) langmuir monolayer, J. Colloid Interface Sci. 325 (2008) 337–345.
[52] A. Pitto-Barry, N.P.E. Barry, Pluronic block-copolymers in medicine: from chemical and biological versatility to rationalization and clinical advances, Polym. Chem. 5 (2014) 3291–3297.
[53] M.Y. Kozlov, N.S. Melik-Nubarov, E.V. Batrakova, A.V. Kabanov, Relationship between Pluronic block copolymer, structure, critical micellization concentration and partitioning coefficients of low molecular mass solutes, Macromolecules 33 (2000) 3305–3313.
[54] M.F. Sohail, M. Rehman, H.S. Sarwar, S. Naveed, O. Salman, N.I. Bukhari, I. Hussain, T.J. Webster, G. Shahnaz, Advancements in the oral delivery of docetaxel: challenges, current state-of-the-art and future trends, Int. J. Nanomed. 13 (2018) 3145–3161.
[55] S. Ketrat, D. Japrung, P. Pongprayoon, Exploring how structural and dynamic properties of bovine and canine serum albumins differ from human serum albumin, J. Mol. Graph. Model. (2020) 98.
[56] A. Oyane, H.M. Kim, T. Furuya, T. Kokubo, T. Miyazaki, T. Nakamura, Preparation and assesment of revised simulated body fluids, J. Biomed. Mater. Res. 65 (2003) 188–195.
[57] S.J. McClellan, E.I. Franses, Effect of concentration and denaturation on adsorption and surface tension of bovine serum albumin, Colloid Surf. B 28 (2003) 63–75.
[58] J.L. Sohl, A.G. Aplittgerber, The binding of coomassie brilliant blue to bovine serum albumin: a physical biochemistry experiment, J. Chem. Educ. 68 (1991) 262–264.
[59] C. Liu, W. Yang, Q. Gao, J. Du, H. Luo, Yi Liu, C. Yang, Differential recognition and quantification of HSA and BSA based on two red-NIR fluorescent probes a, J. Lumin. 197 (2018) 193–199.
[60] Y. Li, G. Yang, Z. Mein, Spectroscopic and dynamic light scattering studies of the interaction between pterodontic acid and bovine serum albumin, Acta Pharm. Sin. B 2 (2012) 53–59.
[61] B. Lorber, F. Fischer, M. Bailly, H. Roy, D. Kern, Protein analysis by dynamic light scattering: methods and techniques for students, Biochem. Mol. Biol. Educ. 40 (2012) 372–382.
[62] R.A. Curtis, J. Ulrich, A. Montaser, J.M. Prausnitz, H.W. Blanch, Protein-protein interactions in concentrated electrolyte solutions, Biotechnol. Bioeng. 79 (2002) 367–380.
[63] S. Servagent-Noinville, M. Revault, H. Quiquampoix, M.H. Baron, Conformational changes of bovine serum albumin induced by adsorption on different clay surfaces: FTIR analysis, J. Colloid Interface Sci. 221 (2000) 273–283, 10.1006/jcis.1999.6576 WOS:000084997300019. PMID: 10631031.
[64] T. Kopac, B.K. ozgeyik, J. Yener, Effect of pH and temperature on the adsorption of bovine serum albumin onto titanium dioxide, Colloid Surf. A 322 (2008) 19–28. WOS:000257129300004.
[65] G. Kutluay, An Investigation of Morphology of Polymeric Micellar Structures in the Presence of Protein for Drug Delivery Purposes (Ms thesis), Izmir Institute of Technology, Department of Chemistry, Urla, Izmir, Turkey, 2017.
[66] U. Ashraf, O.A.M. Chat Maswal, S. Jabeen, A. Dar Ahmad, An investigation of Pluronic P123–sodium cholate mixed system: micellization, gelation and encapsulation behavior, RSC Adv. 5 (2015) 83608–83618.
[67] A. Raval, S.A. Pillai, A. Bahadur, P. Bahadur, Systematic characterization of Pluronic micelles and their application for solubilization and in vitro release of some hydrophobic anticancer drugs, J. Mol. Liq. 230 (2017) 473–481.
[68] E. Cihan, M. Polat, H. Polat, Designing of spherical chitosan nano-shells with micellar cores for solvation and safeguarded delivery of strongly lipophilic drugs, Colloids Surf. A Physicochem. Eng. Asp. 529 (2017) 815–823.
[69] C. Farace, P. Sánchez-Moreno, M. Orecchioni, R. Manetti, F. Sgarrella, Y. Asara, M. José, P. García, J.A. Marchal, R. Madeddu, L.G. Delogu, Immune cell impact of three differently coated lipid nanocapsules: Pluronic, chitosan and polyethylene glycol, Nat. Sci. Rep. 6 (2016) 18423.
[70] K. Dehvari, K.S. Lin, B. Hammoud, Small-angle neutron scattering studies of microenvironmental and structural changes of Pluronic micelles upon encapsulation of paclitaxel, J. Taiwan Inst. Chem. Eng. 71 (2017) 405–413.